JOURNAL OF BIOMOLECULAR STRUCTURE AND DYNAMICS
https://doi.org/10.1080/07391102.2021.1886991

In silico prediction of SARS-CoV-2 main protease and polymerase inhibitors: 3D-Pharmacophore modelling

Mona Mosayebnia[a], Atefeh Hajiagha Bozorgi[b]*, Maliheh Rezaeianpour[c] and Farzad Kobarfard[a]

[a]Department of Radiopharmacy and Pharmaceutical Chemistry, School of Pharmacy, Shahid Beheshti University of Medical Sciences, Tehran, Iran; [b]Department of Medicinal Chemistry, Faculty of Pharmacy, Alborz University of Medical Sciences, Karaj, Iran; [c]Chronic Respiratory Diseases Research Center, National Research Institute of Tuberclosis and Lung Diseases (NRTLD), Shahid Beheshti University of Medical sciences, Tehran, Iran

Communicated by Ramaswamy H. Sarma

ABSTRACT

The outbreak of the second severe acute respiratory syndrome coronavirus (SARS-CoV-2) known as COVID-19 has caused global concern. No effective vaccine or treatment to control the virus has been approved yet. Social distancing and precautionary protocols are still the only way to prevent person-to-person transmission. We hope to identify anti-COVID-19 activity of the existing drugs to overcome this pandemic as soon as possible. The present study used HEX and AutoDock Vina softwares to predict the affinity of about 100 medicinal structures toward the active site of 3-chymotrypsin-like protease (3Clpro) and RNA-dependent RNA polymerase (RdRp), separately. Afterwards, MOE software and the pharmacophore-derived query methodology were employed to determine the pharmacophore model of their inhibitors. Tegobuvir (**19**) and compound **45** showed the best binding affinity toward RdRp and 3Clpro of SARS-CoV-2 in silico, respectively. Tegobuvir -previously applied for hepatitis C virus- formed highly stable complex with uncommon binding pocket of RdRp (E total: −707.91 Kcal/mol) in silico. In addition to compound **45**, tipranavir (**28**) and atazanavir (**26**) as FDA-approved HIV protease inhibitors were tightly interacted with the active site of SARS-CoV-2 main protease as well. Based on pharmacophore modelling, a good structural pattern for potent candidates against SARS-CoV-2 main enzymes is suggested. Re-tasking or taking inspiration from the structures of tegobuvir and tipranavir can be a proper approach toward coping with the COVID-19 in the shortest possible time and at the lowest cost.

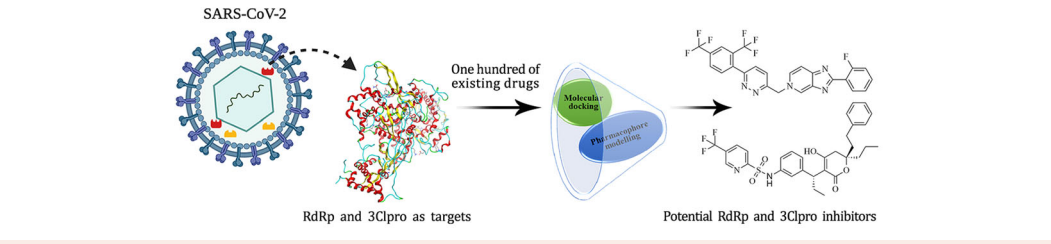

Abbreviations: AIDS: Acquired immunodeficiency syndrome; AR: Aromatic ring; 3Clpro: 3-Chymotrypsin-like protease; CoVs: Coronaviruses; COVID-19: Coronavirus Disease 2019; FDA: Food and drug administration; HBA: Hydrogen bond acceptors; HBD: Hydrogen bond donors; HCV: Hepatitis C virus; HIV: Human immunodeficiency virus; HY: Hydrophobic centers; MERS-CoV: Middle East respiratory syndrome coronavirus; Mpro: Main protease; NSPs: Non-structural proteins; PDQ: Pharmacophore-derived query; PI group: Positive ionizable group; RdRp: RNA-dependent RNA polymerase; SARS-CoV-2: Severe acute respiratory syndrome coronavirus-2; ssRNA viruses: Single-stranded RNA viruses; ZIKV: Zika virus

ARTICLE HISTORY
Received 5 October 2020
Accepted 2 February 2021

KEYWORDS
SARS-CoV-2; protease 3Clpro; RdRp; docking study; pharmacophore modelling

1. Introduction

Coronaviruses (CoVs) are life-threatening infective agents of respiratory system which have erupted since 1960 (Chen et al., 2020). The highest mortality rate associated with CoVs has been reported to be 34.4% (Petrosillo et al., 2020). They belong to enveloped, positive-sense, single-stranded RNA viruses (+ssRNA) which were named corona-virus owing to their surface glycoproteins with crown-like appearance. Generally, the CoVs are classified into four categories: alpha,

CONTACT Mona Mosayebnia m_mosayebnia@sbmu.ac.ir Department of Radiopharmacy and Pharmaceutical Chemistry, School of Pharmacy, Shahid Beheshti University of Medical Sciences, Niayesh junction, Vali-e-Asr Ave, Tehran, 14155-6153, Iran
*Present address: Evidence-based Phytotherapy and Complementary Medicine Research Center, Alborz University of Medical Sciences, Karaj, Iran.

beta, gamma, delta (Chan et al., 2013; Perlman & Netland, 2009). The severe acute respiratory syndrome coronavirus (SARS-CoV) and the Middle East respiratory syndrome coronavirus (MERS-CoV) from beta group are two main causes of severe pneumonia transmitted from animals to humans (Hoffmann et al., 2020). The SARS-coronavirus 2 (SARS-CoV-2) is the 7th of the new CoVs called as "COVID-19" emerged from Chinese sea-food market in late 2019 (Huang et al., 2020; Zhu et al., 2020). Despite the high genetic similarity (>80%) between COVID-19 and SARS-CoV, COVID-19 is more contagious via aerosol particles and fecal-oral route (Chan et al., 2020; Jia et al., 2005). This is probably due to its higher binding affinity (10-20 times) toward host cell receptors (Wrapp et al., 2020), long latent period of disease (~10 days) (Li et al., 2020) and mild symptoms of patients in the early-stages of infection (Chen et al., 2020; Tang et al., 2020). Currently, minimizing the exposure to the virus is the only available approach to control the spread of COVID-19. It is estimated that each infected individual can transmit the infection to > 2 healthy persons (Fauci et al., 2020). Economic losses and lack of an approved vaccine and an effective drug have encouraged the researchers to eradicate this virus as soon as possible (Enjuanes et al., 2006; Perlman & Netland, 2009).

Vaccination is a certain way to save people but it takes a long time to prepare and distribute vaccines around the world (Ahmed et al., 2020). So, many attempts are currently focused on drug repurposing against COVID-19. Drug repurposing is a strategy to identify new uses for pre-existing drugs which can be prescribed for rapid coping with the emerging disease at the lowest cost. There are different targets encoded by viral genome including structural and non-structural proteins for designing effective drugs. Structural proteins like the capsid spike glycoprotein (S), Nucleocapsid (N) Matrix (M) and Envelope (E) have been usually considered for designing targeted monoclonal antibodies (mAbs) and vaccines (Ahmed et al., 2020; Elfiky, 2020). The COVID-19 takes advantage of non-structural proteins (NSPs) to maintain its survival. The 3-chymotrypsin-like protease (3Clpro or Mpro), papain-like protease (Plpro) and RNA-dependent RNA polymerase (RdRp) are three crucial NSPs with enzymatic functions in the COVID-19 life cycle (Morse et al., 2020). The 3Clpro is a cysteine proteases which produces functional units for the virus transcription and replication process in the host cells (Sheahan et al., 2020). The RdRp (NSP_{12}) is an indispensable enzyme in maturation cycle of RNA viruses like hepatitis C virus (HCV), zika viruses (ZIKV) and CoVs (Elfiky, 2020). It has a large deep groove for replication of RNA from an RNA template (Morse et al., 2020). So, these NSPs have provided an opportunity for rational design of the structure-based inhibitors. Preliminary studies have introduced the numbers of protease and RdRp inhibitors presumably applied in COVID-19 treatment. For instance, The kaletra® is a combination medication of two HIV protease inhibitors (lopinavir + ritonavir) examined as an option to treat coronavirus disease (Cao et al., 2020; Chandwani & Shuter, 2008). Ribavirin and Sofosbuvir are also other examples of COVID-19 RdRp inhibitors previously approved by FDA for HCV treatment (Elfiky, 2020; Elfiky & Ismail, 2019; Yang et al., 2011). The protease "3Clpro or Mpro" and polymerase "RdRp" are two pivotal enzymes required for COVID-19 replication which are 96% similar to the SARS-CoV. That is why the drugs targeting SARS-Cov RdRp and 3Clpro can be considered as presumable compounds with anti-COVID-19 activity (Morse et al., 2020). The aim of this study is to compare large numbers of existing inhibitors of RdRp (Table 1) and 3Clpro (Table 2) obtained by literature mining in silico to identify the best pharmacophores and drug candidates against SARS-CoV-2. We hope that our contribution can offer a suitable pharmacophore or agent for further studies. The flowchart of the present study is described in Figure 1.

2. Materials and methods

2.1. Creation of compound databases

Based on literature review, a compound database including existing drugs with different mechanisms (antiviral, anthelmintic agents and etc.) was firstly provided for molecular docking studies. In the present study, the main protease (3Clpro/Mpro) and RNA polymerase (RdRp) of COVID-19 were considered as targets of these drugs. Different types of RdRp inhibitors including nucleoside, nucleotide and non-Nucleoside compounds were evaluated in silico. The peptidomimetics and small molecules were docked on the binding pocket of 3Clpro as well. Out of the existing drugs, the drugs targeting protease and RNA polymerase in other RNA viruses with one of the following features were certainly selected for further experiments: 1) FDA-approved agents; 2) The drugs under investigation with better antiviral activity and less cytotoxicity. The half maximal effective concentration (EC_{50}) and half maximal inhibitory concentration (IC_{50}) values were considered as useful parameters to judge the effectiveness of these viral replication inhibitors. The protease and RNA polymerase inhibitors with the lowest EC_{50} or IC_{50} were chosen accordingly. To generate ligands, the two-dimensional (2 D) chemical structures of the inhibitors were drawn and saved in mol. format at first. Our compound database was then constructed in 3 D structure of molecules using Hyperchem Software. Energy of ligands was minimized by using MM + force field and the Polak-Ribiere algorithm until the root mean square (RMS) gradient was 0.01 kcal/mol. Then all structures were saved as pdb. files and utilized in docking studies.

2.2. Preparation of target proteins

The protein structures of SARS-CoV-2 RdRp (PDB ID: 6M71) and 3Clpro (PDB ID: 6LU7) were obtained from protein data bank (https://www.rcsb.org) in pdb. format with good resolutions. In the case of the 6LU7 and 6M71 proteins, chain A was chosen as a receptor for docking analysis. The protein preparation protocol was executed using AutoDockTools in several steps: 1) Removing the native ligand and water molecules from pdb. file, 2) Adding polar hydrogen atoms and Kollman charges, 3) Merging nonpolar hydrogen atoms, and

Table 1. Chemical structures and classifications of some existing inhibitors of RdRp.

RdRp inhibitors	Class	Structure
	Nucleoside	
Ribavirin (**1**)	Guanosine analog	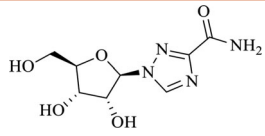
2	7-deaza-6,7-disubstituted adenosine analog	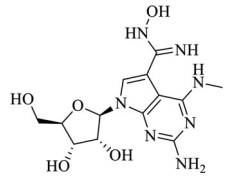
3	4′-Azidocytidine	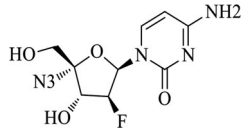
RG7128 (**4**)	2′-F, 2′-methyl cytidine	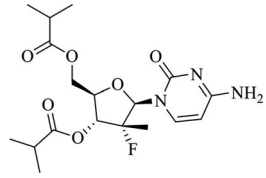
	Nucleotide	
Remdesivir (**5**)	1′-cyano-C-adenosine PA[a]	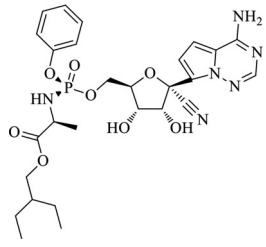
IDX184 (**6**)	2′-OH, 2′-methyl guanosine PA	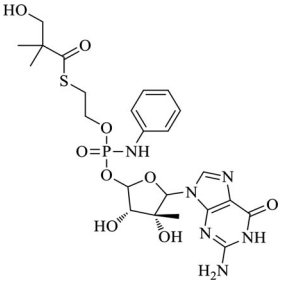
INX-08189 (**7**)	2′-OH, 2′-methyl guanosine PA	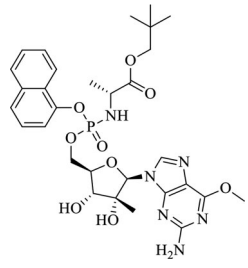

(*continued*)

Table 1. Continued.

RdRp inhibitors	Class	Structure
	Nucleoside	
Sofosbuvir (**8**)	2′-F-2′-methyl uridine PA	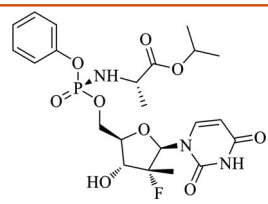
	Non-nucleoside	
Favipiravir (**9**)	Pyrazinecarboxamide	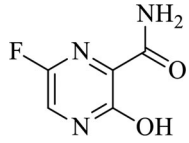
10	Benzothiadiazine	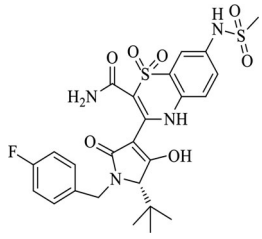
11	Benzothiadiazine	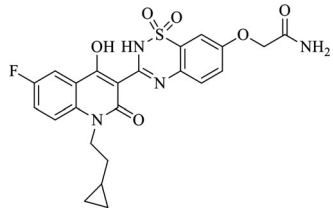
JTK-109 (12)	Benzimidazole	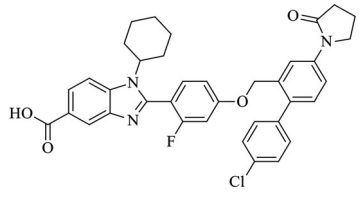
13	Benzimidazole	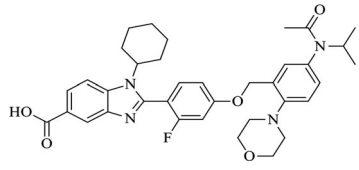
14	Indole	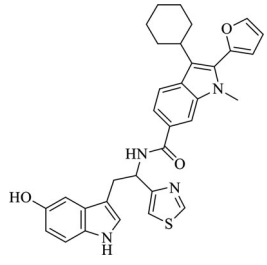
15	Benzodiazepinoindole (multicyclic)	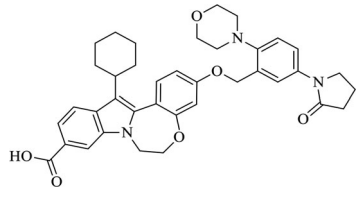

(*continued*)

Table 1. Continued.

RdRp inhibitors	Class	Structure
	Nucleoside	
16	Benzoazepine (multicyclic)	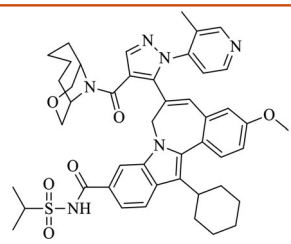
17	Dihydropyrone	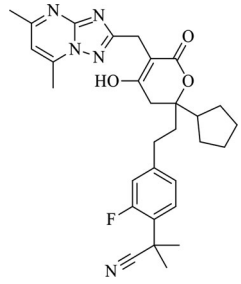
18	Quinolone	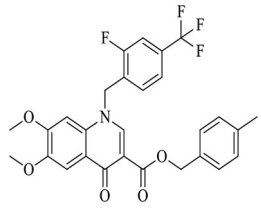
Tegobuvir (**19**)	Imidazolopyridine	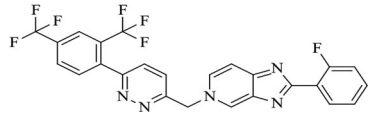

[a)]PA: 5′-PhosphorAmidate.

4) Assigning AutoDock 4 atom type to the protein structure. Finally, the prepared files were saved in PDBQT format. The characteristics of 3CLpro and RdRp crystallographic structures are summarized in Table 3.

2.3. Molecular docking

Docking screening is a valuable method for drug design which predicts the affinity of generated ligands to the essential residues in the active site of receptor or enzyme (Carlesso et al., 2019). After preparation of the ligands and target proteins, all presumable molecules were subjected to the HEX docking software. The Parameters for docking was set as follows: Correlation type: Shape + Electro + Dars Grid dimension: 0.6, Receptor range: 180, Ligand range: 180, Distance range: 40, Box size: 10. Afterwards, the best docking results obtained by HEX software, were docked using AutoDock Vina software to recheck their binding affinity toward main enzymes of COVID-19 as well. Flexible ligand docking analyses were used.

2.4. Pharmacophore model extraction using MOE

To provide a pharmacophore profile of 3Clpro and RdRp inhibitors and lead compounds, pharmacophore query methodology was used. For this purpose, an MOE database was created and up to 2500 different conformations of molecules were prepared. Using pharmacophore query tool, a pharmacophoric map of enzymes inhibition is obtained separately. This method is based on searching 3 D distances between overlapped binding centers like hydrogen bond donors (HBD)/acceptors (HBA), positive ionizable (PI) group, aromatic ring (AR) and hydrophobic centers (HY) in the structure of ligand-receptor complexes (Pickett et al., 1996). Accordingly, some new platforms were designed and suggested as potential candidates for inhibition of 3Clpro/Mpro and RdRp of COVID-19.

3. Results

3.1. Molecular docking

As there is no available therapeutic agent to efficiently treat COVID-19 so far; docking studies can be a favorable

TABLE 2. Chemical structures and indications of some existing protease inhibitors.

Protease inhibitors	Structure	Indication
Darunavir (**20**)	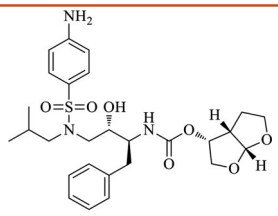	Anti-HIV[a]
Ritonavir (**21**)	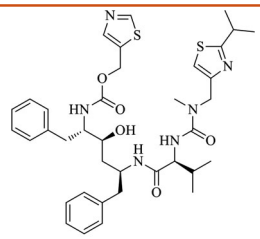	
Lopinavir (**22**)	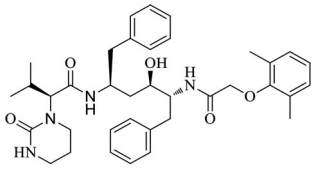	
Indinavir (**23**)	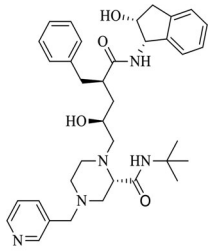	
Fosamprenavir (**24**)	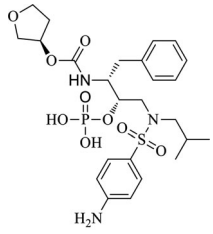	
Nelfinavir (**25**)	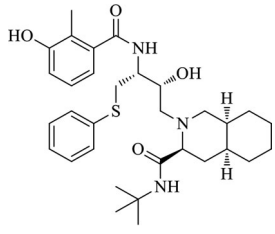	
Atazanavir (**26**)	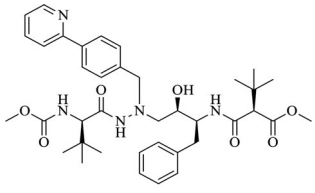	
Amprenavir (**27**)	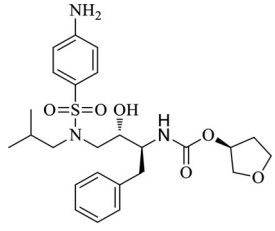	
Tipranavir (**28**)	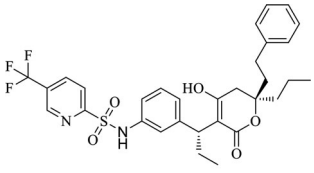	
PD-178390 (**29**)	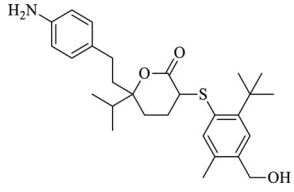	
JE-2147 (**30**)	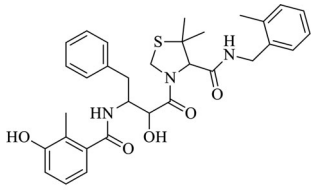	Anti-HIV
JE-533 (**31**)	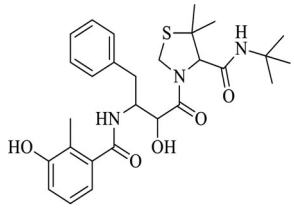	
		Anti-HCV[b]

(*continued*)

TABLE 2. Continued.

Protease inhibitors	Structure	Indication
Simeprevir (**32**)	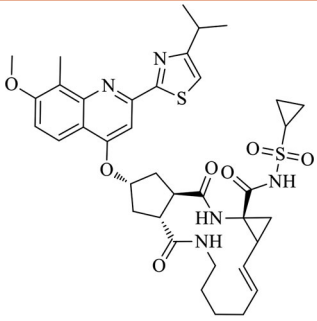	
Boceprevir (**33**)	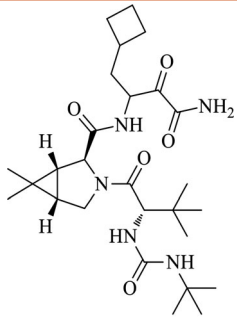	
Asunaprevir (**34**)	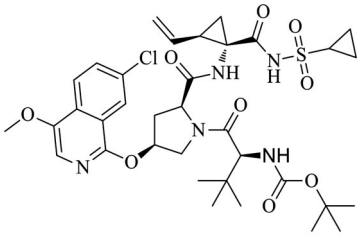	
Niclosamide (**35**)	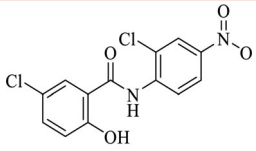	Anthelmintic
Nitazoxanide (**36**)	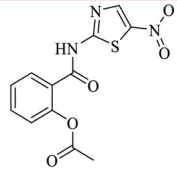	
NPI-64 (**37**)	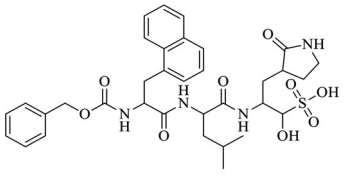	Anti-Feline CoV
GC-376 (**38**)	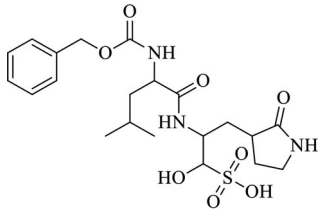	
39	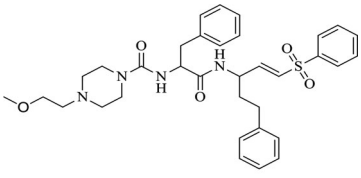	Anti-SARS-CoV
40	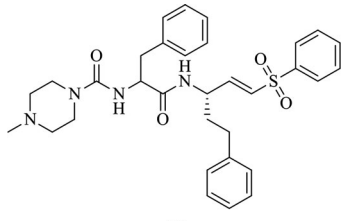	
41	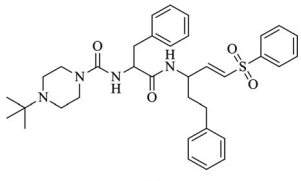	
Xanthoangelol D (**42**)	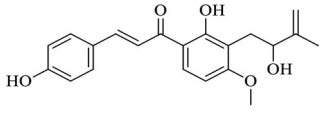	

(*continued*)

TABLE 2. Continued.

Protease inhibitors	Structure	Indication
KZ7088 (**43**)	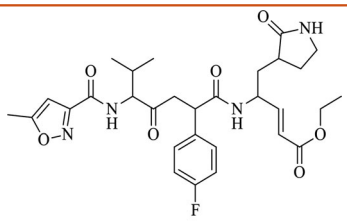	
44	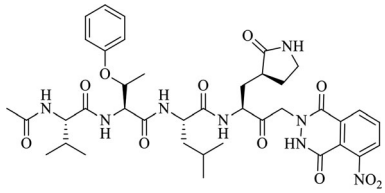	
44	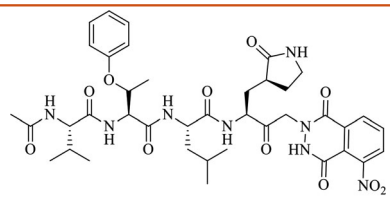	

[a)]HIV: Human Immunodeficiency Viruses/[b)] HCV: Hepatitis C Virus.

approach to find potential candidates. Over 100 structures either available in the market or under development have been screened in this survey. Their interactions with binding pocket of SARS-CoV-2 main enzymes (3Clpro PDB: 6LU7 and RdRp PDB: 6M71) were assessed. Presumable agents including many FDA-approved and under-construction antiviral or anthelmintic agents specifically anti-RNA-virus drugs were docked and the most stable inhibitor-enzyme complexes were selected based on the range of E total (free energy of binding) values.

All docked molecules on the active sites of RdRp and 3Clpro showed negative binding energies ranging from −161.28 to −707.91 kcal/mol and −216.9 to −415.27 kcal/mol, respectively. The top 25 agents including 15 RdRp inhibitors and 10 protease inhibitors with the best E total value are shown in Table 3. The binding affinity of all 25 top molecules were analyzed using AutoDock Vina software and represented as well (Table 4).

The docking results exhibited that the order of E total in RdRp inhibitors was as follows: non-nucleoside < nucleotide < nucleoside compounds which were properly correlated with the energy of binding obtained by AutoDock Vina. The binding pocket for non-nucleoside inhibitors were notably different from nucleoside and nucleotide inhibitors in the enzyme structure (Figure. 2). All nucleoside and nucleotide inhibitors were accommodated in the common polymerase active site depicted in a yellow circle in Figure 2. In 1999, the presence of various subdomains of “palm”, “fingers”, and “thumb” has been reported in the crystallographic structure of different polymerases, too (Sofia et al., 2012).

Out of the non-nucleoside inhibitors, tegobuvir (**19**) was tightly interacted with uncommon RdRp binding pocket (E total: −707.91 kcal/mol). This imidazolopyridine-based agent has been docked on the NS5B polymerase of HCV and introduced as its thumb site inhibitor. Tegobuvir also inhibited hepatitis C virus nonstructural protein 5B (NS5B) polymerase at a low concentration (EC_{50} = 0.0007 μM toward genotype 1 b, EC_{50} = 0.0025 μM toward genotype 1a HCV polymerase) in vitro (Sofia et al., 2012). As expected, tegobuvir was accommodated somewhere out of common binding pocket of RdRp enzyme structure illustrated in Figure 3A. The fluorine atoms in tegobuvir formed an extensive network of H-bonds with the acceptor residues of hydrogen bonds including Thr123 (2.80 Å), Tyr217 (3.16 Å), Thr120 (4.30, 4.93 Å), Thr206 (4.92 Å), and Arg33 (5.03 Å). The hydrophobic bound with Tyr217 (3.06 Å) and Phe35 (3.91 Å) residues result in stabilizing the ligand-receptor complex as well (Figure. 3B). Tegobuvir (GS-9190) by itself and in combination with other anti-HCV drugs were assessed in some clinical trials and showed high potency in viral load reduction with no significant cytotoxicity (Wyles et al., 2014). It is under active investigation though.

In the case of nucleotide inhibitors, INX-08189 (**7**) interacted with RdRp active site stronger than sofosbuvir and remdesivir in a row (E total∼ −396 kcal/mol)) (Figure. 4A). Although sofosbuvir (**8**) formed three hydrogen bonds with Tyr129 (3.16 Å), Asn781 (3.22 Å) and Lys780 (3.46 Å) residues of enzyme, INX-08189 (**7**) showed better binding properties probably owing to a strong H-bond with the Tyr129 residue at a closer distance (2.20 *Vs.* 3.16 Å) (Figure. 4B). It should be noted that INX-08189, sofosbuvir and remdesivir are overlaid in the active site (Figure. 4B). Remdesivir (**5**) was also accommodated into the active site via a hydrogen and cation − π bonding with Gln773 (3.33 Å) and Lys47 (3.40 Å), respectively. Meanwhile, INX-08189 and sofosbuvir have been examined in HCV-positive patients during clinical trials (Han et al., 2019; Sofia, 2011).

Nucleoside inhibitors were not as good as nucleotide inhibitors in terms of binding energies. Out of them, RG7128 (**4**) manifested the lowest E total value (Figure. 5).

The ranking of E total for protease inhibitors revealed that the best docking score (E total of ~ −400 kcal/mol or lower) belongs to compound **45**, tipranavir (**28**), **44** and atazanavir (**26**) in a row (Figure 6). Their interaction profiles of the best-docked poses are also illustrated in Figure 7. The carbonyl groups of compound **45** interacted by forming hydrogen bonds with amino acid Ser46 (2.04 Å) and Cys145 (3.75 Å). A pi-pi bonding was also visible between His41 and aromatic ring at a distance of 3.95 Å. Tipranavir was bound to the 3Clpro active site via amino acid His41 (1.53 Å) and His163 (2.32 Å) as well. As shown in Figure. 7C, compound (**44**) formed three hydrogen bonds with the side chain of Asn142 (2.23, 3.19 Å) and Ser46 (3.22 Å). Atazanavir (**26**) showed same hydrogen bonding with Asn142 (3.57 Å) as that of compound (**44**). Additionally, Met49 and Cys145 were interacted with atazanavir via weak H-bonding. It is noteworthy that tipranavir and atazanavir have shown potent activity in the HIV replication assay and in improving quality of life of patients with HIV/AIDS (Lv et al., 2015). The agents **45** and **44** have already reported as peptidomimetics reversibly inhibited SARS-CoV (Pillaiyar et al., 2016).

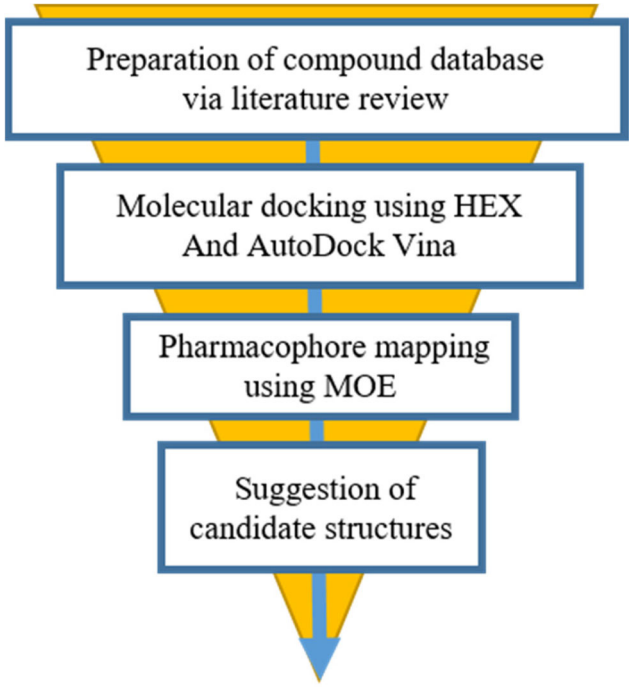

Figure 1. The flowchart of the present in-silico study.

3.2. Pharmacophore model extraction

Using MOE software, a pharmacophoric map of the RdRp- and 3Clpro-inhibitors was generated. The key common contributing features with inter-features distances of these inhibitors are shown in Figure 8. As shown in the Figure. 8A, a 2 D pharmacophore model for the RdRp inhibitors consists of a HY center connected to another HY via an HBA. The distance between two hydrophobic regions is 3.91 A°. Two RA centers aligned to each other, leading to a HY center, is the rest of the pharmacophoric map of RdRp inhibitors. The length of this section is 4.12 A°. It seems that the inhibitors had better have a planar structure without any harsh angles.

In the case of 3Clpro inhibitors, HY centers which are connected to aromatic regions play an important role in binding to the enzyme. Having HBA/HBD group help the inhibitor to bind tightly to enzyme. 90° angles in the structures show that the inhibitors do not have linear structures (Figure. 8B).

4. Discussion

Considering the mortality rate and the socio-economic complications associated with the outbreak of new CoVs, there is an urgent need to finding a quick solution for this global threat. As of December 2019, some antiviral and anti-parasitic drugs have been applied to relieve COVID-19 symptoms. It is assumed that the existing drugs can be used as off-label treatment of the virus. The 3Clpro and RdRp are critical enzymes in the life cycle of COVID-19 which are 96% similar to the SARS-CoV (Morse et al., 2020). In the present study, we used the crystal structure of 3Clpro/Mpro and RdRp of COVID-19 as receptors for docking analysis on the existing drugs. Many FDA-approved and under-construction antiviral or anthelmintic agents specifically anti-RNA-virus drugs were assessed in silico to find potential candidates to hamper replication of SARS-CoV-2. Actually, our goal was to re-task the existing drugs against COVID-19.

TABLE 3. The characteristics of 3CLpro and RdRp crystallographic structures.

Target	PDB code	Resolution (A°)	Native Ligand	Main residues of chain A	Ref.
3ClPro	6LU7	2.16	N-[(5-methylisoxazol-3-yl)carbonyl]alanyl-l-valyl-*N*~1~-((1R,2Z)-4-(benzyloxy)-4-oxo-1-{[(3R)-2-oxopyrrolidin-3-yl]methyl}but-2-enyl)-L-leucinamide	Thr24, Thr26, Phe140, Asn142, Gly143, Cys145, His163, His164, Glu166, His172	(Jin et al., 2020)
RdRp	6M71	2.90	–	Tyr32, Lys47, Tyr122, Tyr129, His133, Asn138, Asp140, Thr141, Ser709, Asn781	(Gao et al., 2020)

Table 4. The top 25 agents inhibiting a RdRp and b 3Clpro of SARS-CoV-2 with the best docking scores.

a) RdRp inhibitors

Compound number[a]	Name	Mw *g/mol*	Reported EC_{50} (IC_{50}) *μM*	E total (Kcal/mol)	Binding affinity (Kcal/mol)	Ref.
2	–	353.33	0.6	−274.53	−7.9	(Sofia et al., 2012)
3	–	286.08	0.024	−291.85	−6.6	(Sofia et al., 2012)
4	RG7128	399.41	2.5	−340.66	−7.8	(Sofia et al., 2012)
5	**Remdesivir**	**602.58**	**0.003-0.79**	**-388.48**	**-9.8**	(Lo et al., 2017)
8	**Sofosbuvir**	**529.16**	**0.014-0.11**	**-396.81**	**-9.3**	(Han et al., 2019)
7	**INX-08189**	**658.64**	**0.01**	**-396.61**	**-10.6**	((Sofia, 2011)
10	–	578.13	0.016	−400.00	−8.8	(Sofia et al., 2012)
17	–	531.62	0.015 (IC_{50} =0.003)	−421.92	−9.7	(Sofia et al., 2012)
11	SB-750330	500.12	0.002 (IC_{50}<0.005)	−430.55	−9.6	(Sofia et al., 2012)
15	–	635.75	0.0076 (IC_{50} =0.0072)	−431.67	−10.6	(Sofia et al., 2012)
16	–	817.01	0.004 (IC_{50} =0.0043)	−448.59	−9.5	(Sofia et al., 2012)
13	–	628.73	0.27 (IC_{50} =0.042)	−480.95	−11.1	(Sofia et al., 2012)
12	JTK-109	638.13	0.32 (IC_{50} =0.017)	−542.26	−10.5	(Hirashima et al., 2006)
18	–	529.48	0.23 (IC_{50} = 0.008)	−549.25	−10.3	(Sofia et al., 2012)
19	**Tegobuvir (GS-9190)**	**517.40**	**0.0007**	**-707.91**	**-10.2**	(Sofia et al., 2012)
b) 3Clpro inhibitors						
32	Simeprevir	735.91	0.008-0.028	−383.69	−7.9	(Izquierdo et al., 2014)
23	Indinavir	611.82	0.0055	−386.65	−6.7	(Lv et al., 2015)
41	–	616.81	(IC_{50}= 0.00006)	−386.66	−6.3	(Morse et al., 2020)
39	–	618.79	(IC_{50}=0.00007)	−387.53	−6.4	(Morse et al., 2020)
22	Lopinavir	628.80	~0.017	−390.02	−6.3	(Lv et al., 2015)
34	Asunaprevir	748.29	0.001-0.004	−395.87	−6	(McPhee et al., 2012)
26	Atazanavir	689.84	0.0026-0.0053	−402.33	−7.2	(Lv et al., 2015)
44	–	806.36	0.6	−414.17	−6.7	(Pillaiyar et al., 2016)
28	**Tipranavir**	**601.68**	**0.03-0.07**	**-415.27**	**-6.8**	(Lv et al., 2015)
45	**-**	**646.28**	**0.34**	**-430.77**	**-6.8**	(Pillaiyar et al., 2016)

a)The chemical structure of these compounds are drawn in the introduction section.

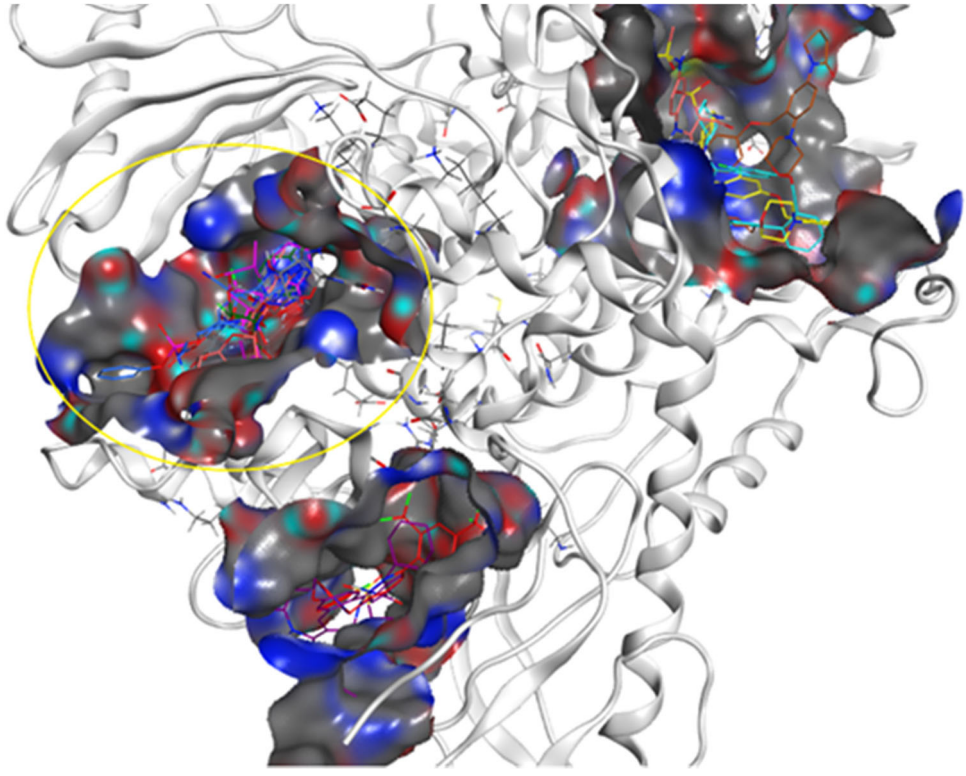

Figure 2. The other binding sites for non-nucleoside RdRp inhibitors removed from the common RdRp binding pocket (shown by yellow circle).

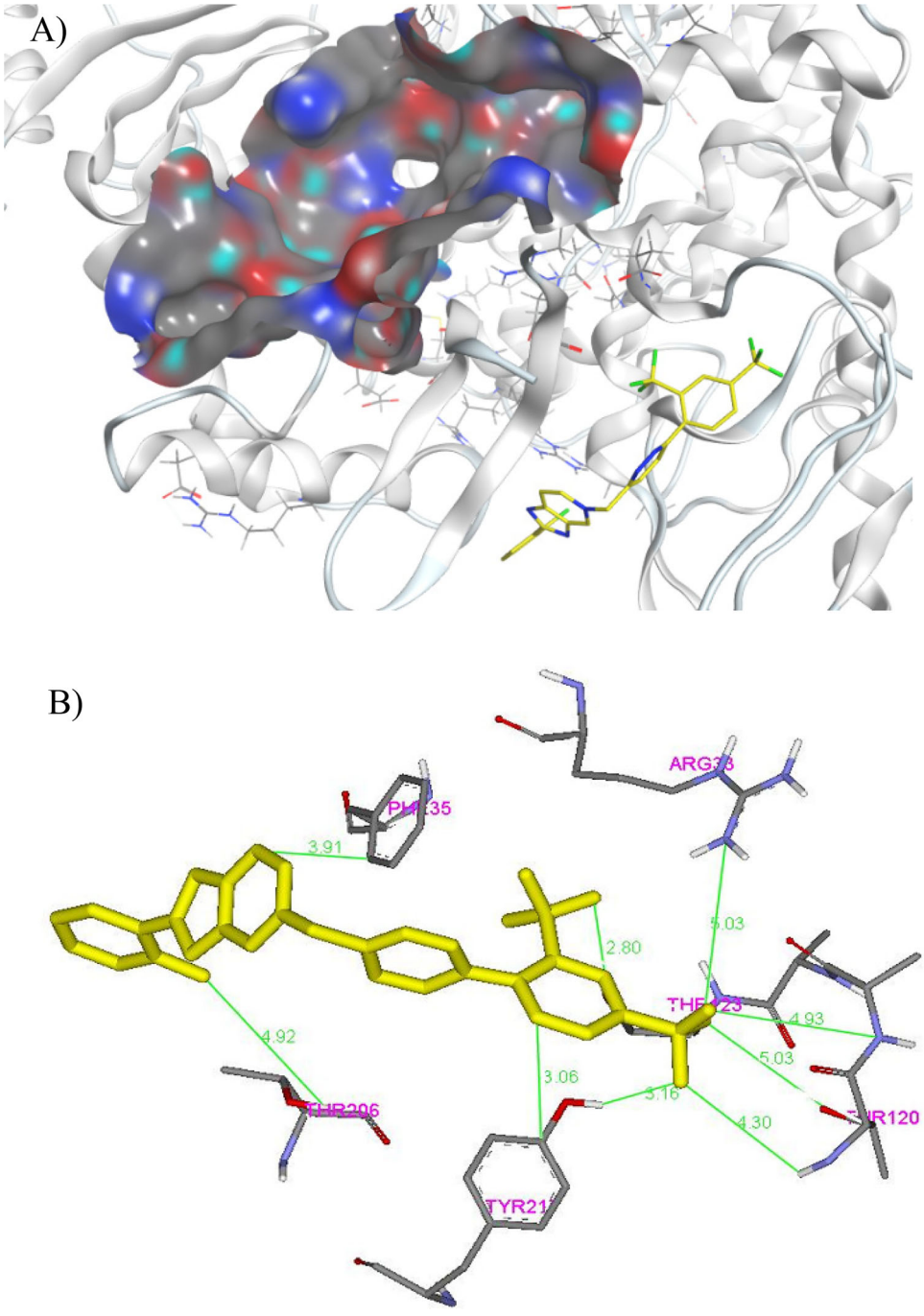

Figure 3. Docked pose of tegobuvir on the crystallographic structure of SARS-CoV-2 RdRp. (A) Tegobuvir (yellow, stick model) are accommodated at the uncommon catalytic site of RdRp. The common main residues are indicated with a blank surface. (B) Docked pose of tegobuvir (yellow, stick model) in interaction with main residues (gray, line model) in the uncommon binding pocket of SARS-CoV-2 RdRp.

Some notable characteristics of approved agents targeting protease and RdRp are summarized in Table 5 and Table 6, respectively. In the case of both groups, there is a relative correlation between reported EC_{50} and calculated E total value for these approved agents. For instance, ribavirin did neither show favorable biding energy against RdRP nor can potently inhibit RNA viruses in vitro and in vivo (Table 5) or anthelmintics drugs with EC_{50} value in the micromolar range didn't show as much inhibition potency as the other protease inhibitors in silico (Table 6) (Wyles et al., 2014).

As illustrated in Table 5, ribavirin did neither show favorable biding energy against RdRP nor can potently inhibit RNA viruses in vitro and in vivo (Sidwell et al., 2005). The best compounds in terms of binding energies proved to be sofosbuvir (**8**) (E total = −396.81 kcal/mol) and then remdesivir (**5**) (E total = −388.48 kcal/mol) which have also shown considerable capability to block hepatitis C and Ebola viruses, respectively. The compound INX-08189 (**7**) had also binding energies of less than −395 kcal/mol which have not been approved by FDA due to its serious cardiomyopathy (Sinokrot et al., 2017).

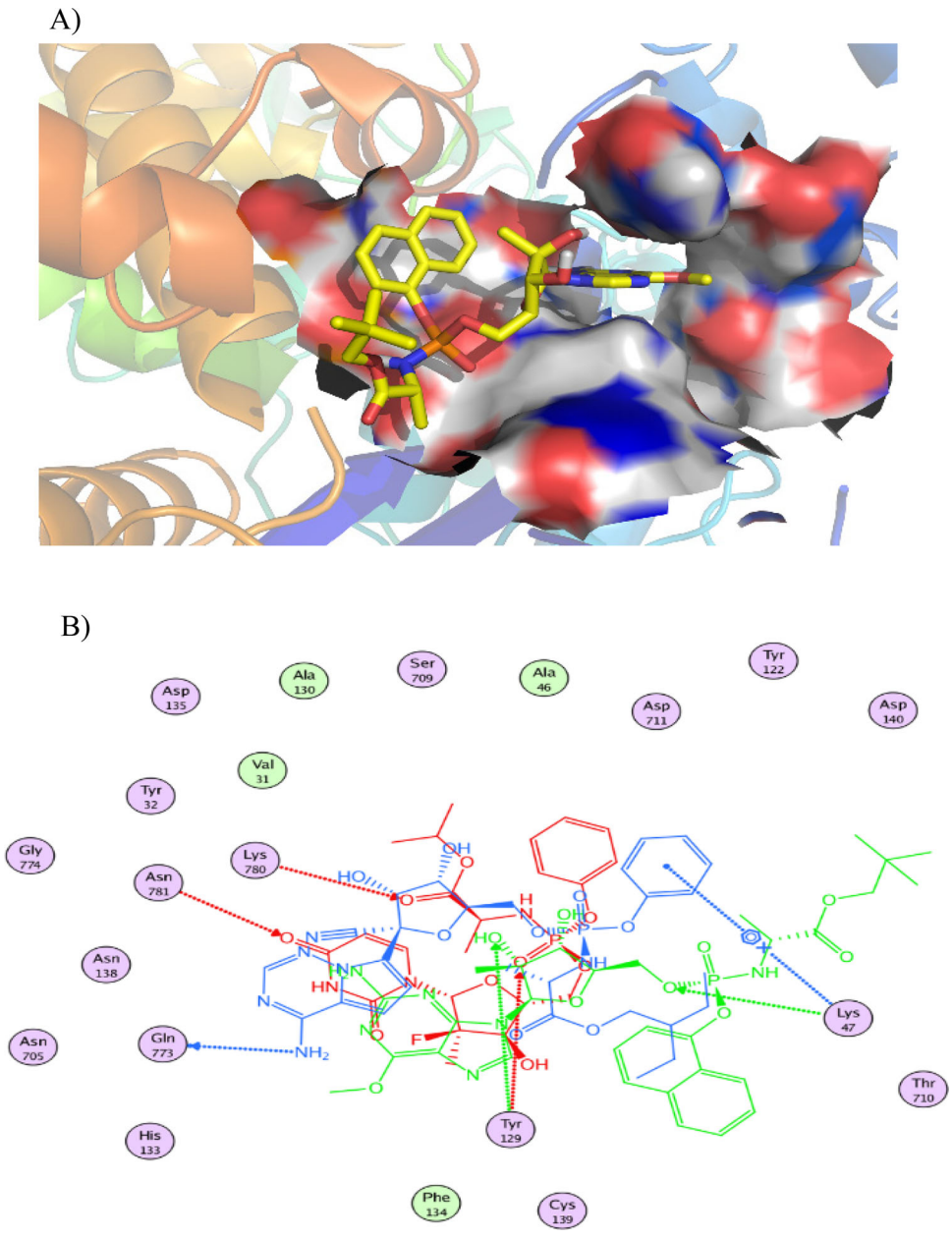

Figure 4. Docked pose of INX-08189 on crystallographic structure of SARS-CoV-2 RdRp. (A) INX-08189 with RdRp of SARS-CoV-2. (B) Overlaid complexes of sofosbuvir (red line), INX-08189 (green line) and remdesivir (blue line) in interaction with main residues in the common active site of RdRp.

It should be noted that in-vitro activity of such drugs as ribavirin, favipiravir, chloroquine, hydroxyquinoline, nitazoxanide, penciclovir and remdesivir against COVID-19 have already been evaluated (Korba et al., 2008; Zhou et al., 2019). Among them, the remdesivir (**5**) exhibited excellent anti-COVID19 activity (EC_{50} = 0.77 μM, CC_{50} > 100 μM) with the highest selectivity index (SI > 129.87) (Korba et al., 2008). Our study revealed that inhibitory potency of INX-08189, sofosbuvir and then remdesivir in silico was also closely correlated with their reported in-vitro and in-vivo antiviral activity. As compared to INX-08189, sofosbuvir and remdesivir are drugs of choice because of their less cytotoxicity. Some clinical studies are underway around the world to assess the safety and efficacy of sofosbuvir and remdesivir in COVID-19 treatment (Eynde, 2020; Sayad et al., 2020). Favipiravir (**9**) has also been studied in some clinical trials as a potential candidate in decreasing the duration of fever and cough of afflicted patients (Malcolm et al., 2006). However, it cannot occupy the active site of RdRp as well as expected owing to its small size or the presence of the other interaction sites. The exact interaction mechanism of favipiravir to RdRp of SARS-Cov-2 can be identified in the future studies.

Based on docking analysis of RdRp inhibitors, Tegobuvir (GS-9190, **19**) can block RdRp of SARS-CoV-2 more efficiently than sofosbuvir and remdesivir. So, tegobuvir may be considered as an appealing clinical candidate to combat COVID-19 since its toxicity profile has been determined during several clinical trials before (Wyles et al., 2014). Definitely, more in-vitro and in-vivo studies are required to confirm its

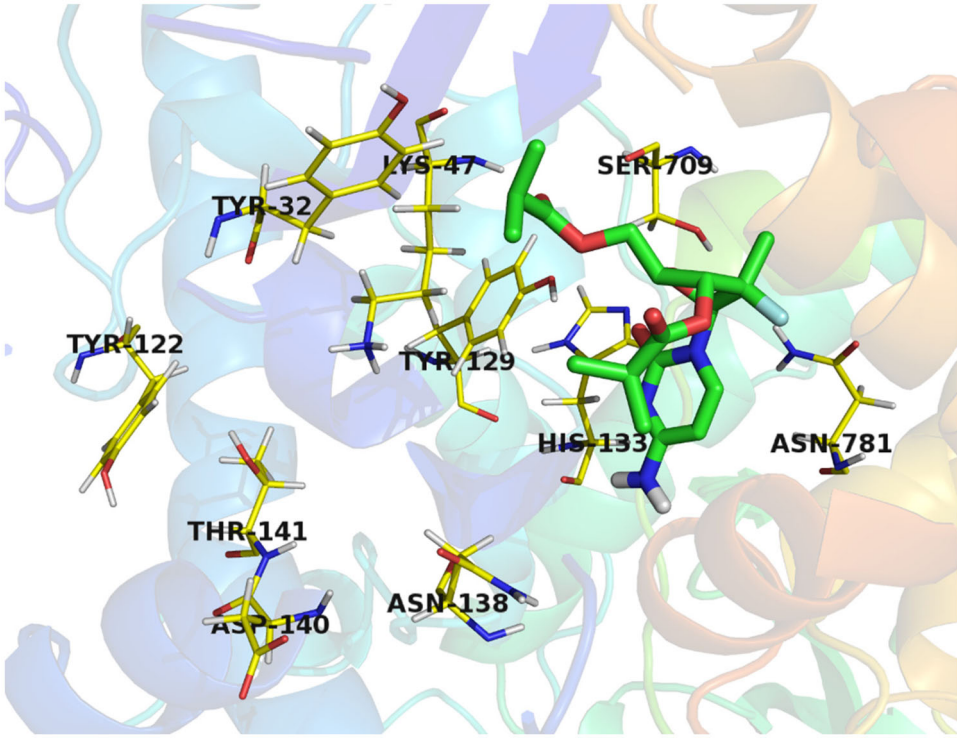

Figure 5. Docked pose of RG7128 (green, stick model) as the best nucleoside inhibitor in the common RdRp catalytic site.

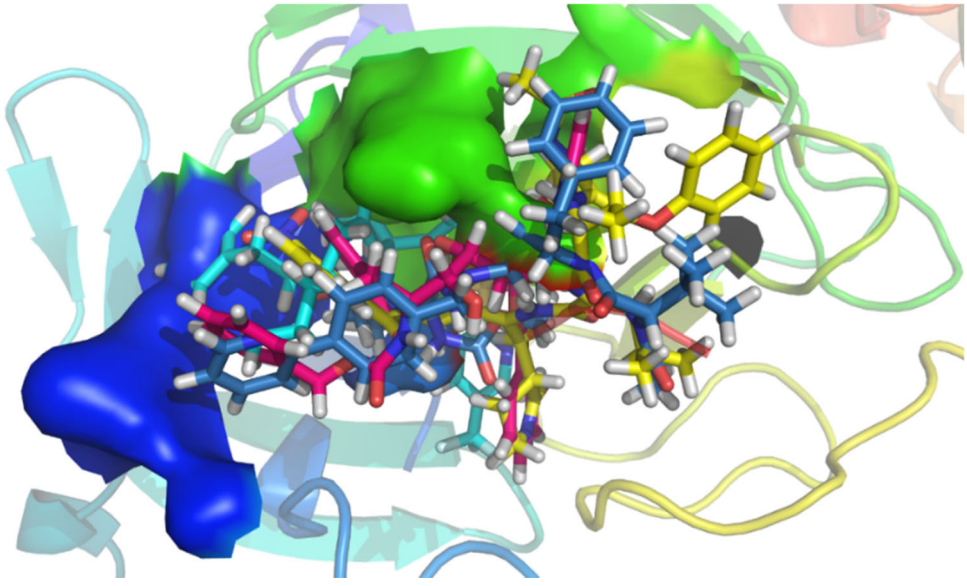

Figure 6. Docked figures of top 4 molecule candidates with 3Clpro active site of SARS-CoV-2. Here, compound **45**, tipranavir (**28**), **44** and atazanavir (**26**) are shown in pink, light blue, yellow and navy blue stick model, respectively.

application against COVID-19. It is noteworthy that oral administration of tegobuvir make it more superior than remdesivir in treatment.

As a result of protease inhibitors, tipranavir **(28)** and atazanavir **(26)** as anti-HIV approved agents and simeprevir **(32)** and asunaprevir **(34)** applied for HCV treatment, manifested hopeful features of binding to the structure of the most important COVID-19 protease. Recently, atazanavir is one of the drug choices in COVID-19 treatment. Finally, we concluded that compound **(45)** and tipranavir **(28)** can form a stable complex with binding pocket of 3Clpro in silico. However, tipranavir with the well-known safety profile may have a bright future in treatment of the present COVID-19 disease (Table 6).

Pharmacophoric mapping is a good approach toward development of drugs in the shortest possible time and with limited resources compared to the conventional

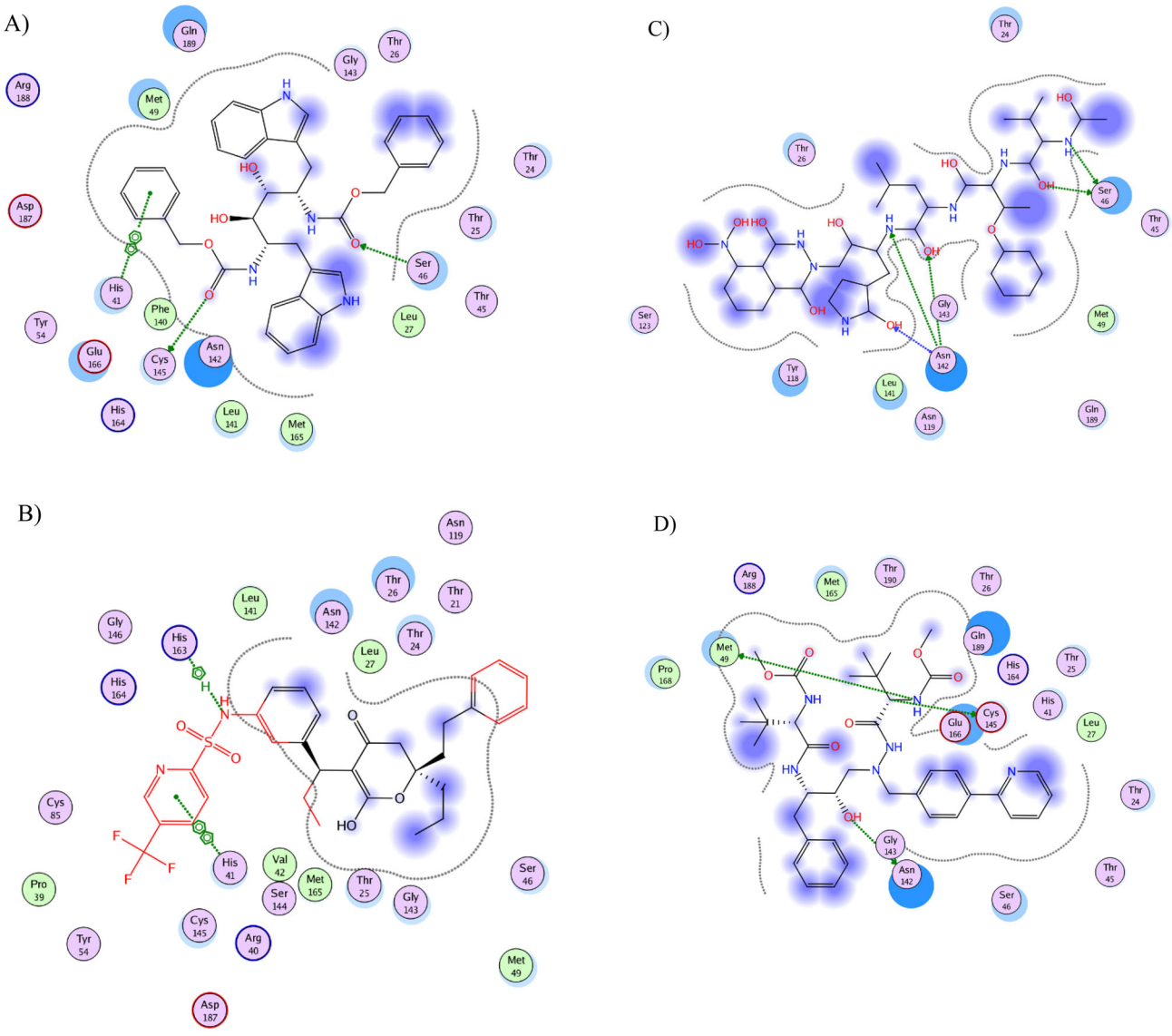

Figure 7. Interaction profile of the best-docked poses of 3Clpro inhibitors. (A) Compound (**45**), (B) Tipranavir (**28**), (C) Compound (**44**) and (D) Atazanavir (**26**).

methods. Utilizing pharmacophore queries in large datasets to find new structures was of critical importance in the last decade (Haji Agha Bozorgi & Zarghi, 2014). By using pharmacophoric features of inhibitors against special targets, one can recognize the importance of each group and interactions between them and the active site in an enzyme structure.

Pharmacophoric map of RdRp inhibitors showed that HY groups (they can be aromatic rings or other ones) play a vital role in their binding properties to this enzyme. Having HBA groups, improve the interaction between inhibitors and active site of the enzyme (Yao et al., 2018; Yin et al., 2020).

Study of the pharmacophoric map of 3Clpro inhibitors revealed that hydrophobic/aromatic regions also have noticeable effect on these class of compounds. Surprisingly, like RdRp inhibitors, HBA/HBD groups can ameliorate their interactions and should be considered as crucial features in the enzyme inhibition (Macchiagodena et al., 2020).

5. Conclusion

In this study, docking procedure was successfully applied to recognize the potential inhibitors of two key enzymes in the life cycle of the SARS-CoV-2, RNA-dependent RNA polymerase (RdRp) and corona virus protease (3Clpro). Docking results showed that tegobuvir (compound number **19**) and sofosbuvir (compound number **8**) as well as remdesivir (compound number **5**) can be potential inhibitors for RdRp enzyme, as a non-nucleoside and nucleotide inhibitors, respectively. Oral administration of tegobuvir make it more superior than remdesivir in treatment though. For inhibition of protease an under-construction molecule with compound

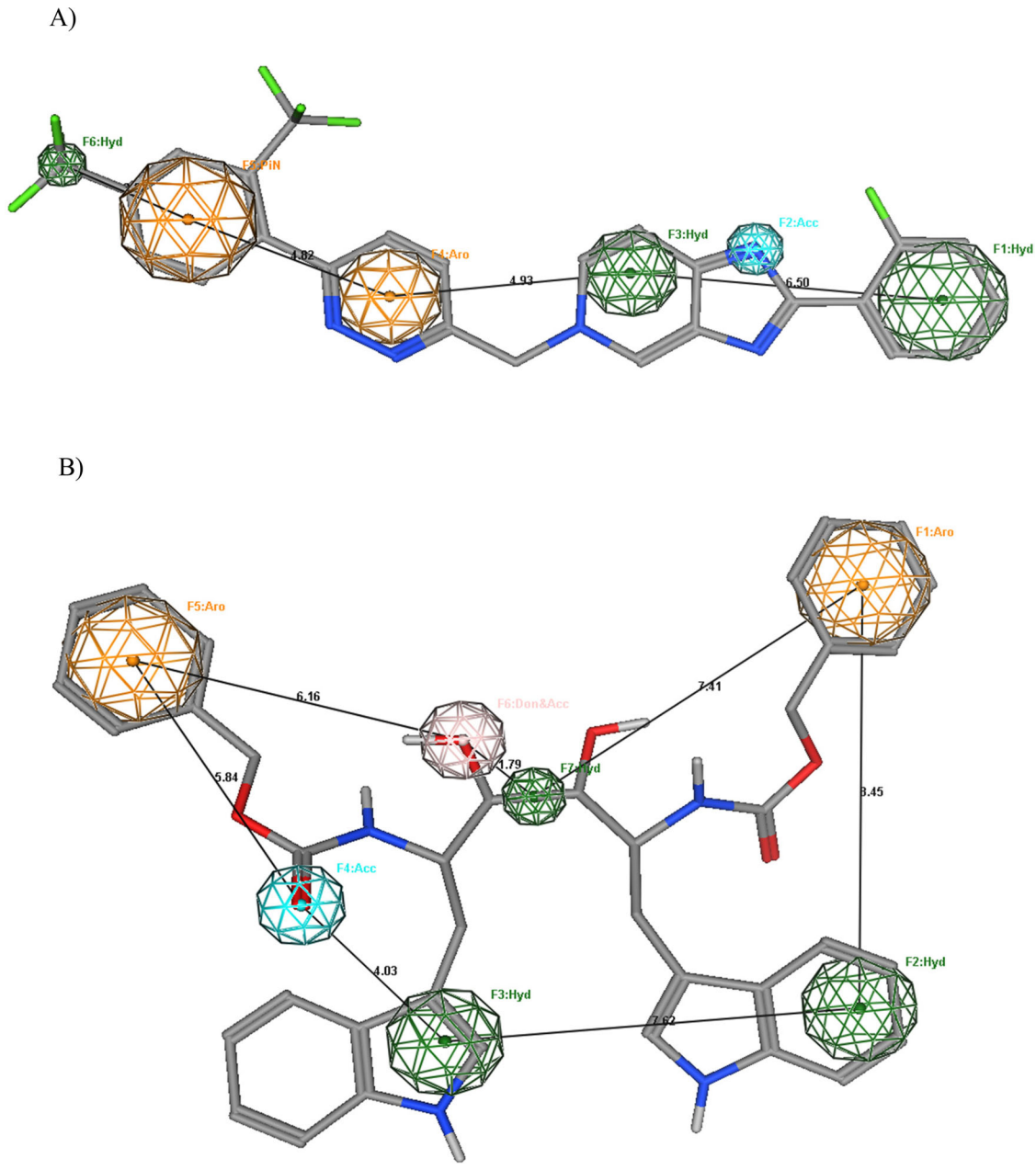

Figure 8. Pharmacophoric maps of the SARS-CoV-2 inhibitors. (A) RdRp inhibitors (B) 3Clpro/Mpro inhibitors with their inter-feature distances. Orange: ring aromatic (RA), Green: Hydrophobic centroid (HY), Blue: H-bond acceptor (HBA), Violet: H-bond donor (HBD), Gray: H-bond donor/acceptor. (HBD/HBA).

Table 5. The characteristics of approved agents inhibiting RdRp.

RdRp inhibitors	Brand name	Year of approval	Indication	EC_{50}	E total (kcal/mol)	Ref.
Ribavirin	Copegus, Rebetol, Ribasphere	1998 (first FDA-approved)	Hepatitis C	~ 0.6-5.5 μM	−207.35	(Sidwell et al., 2005)
Sofosbuvir	Sovaldi	2013	Chronic Hepatitis C	14-110 nM	−396.81	(Han et al., 2019)
Favipiravir	Avigan	approved in Japan in 2014	Influenza A/B/C	0.01-3.53 μM	−197.46	(Furuta et al., 2017)
Remdesivir	GS-5734	–	Ebola virus Marburg, Yellow Fever and Zika viruse infections	0.003-0.79 μM (12 nM for Ebola)	−388.48	(Lo et al., 2017; McMullan et al., 2019)

number **45** and FDA-approved agent tipranavir (compound number **28**) are good enough to be investigated more precisely in COVID-19 treatment. In the next step of present study, pharmacophoric maps of two vital COVD-19 enzymes were achieved using a large compound database obtained through literature mining. Thanks to virtual drug design

Table 6. The characteristics of FDA-approved agents inhibiting proteases of RNA-viruses.

Protease inhibitors	Brand name	Year of FDA approval	Indication	EC_{50}	E total (kcal/mol)	Ref.
Niclosamide	Niclocide	1982	Tapeworm infestations	0.1-2 μM	−216.29	(Wei et al., 2018; Xu et al., 2020)
Saquinavir	Invirase Fortovase	1995	HIV infection	37.7 nM	−378.3	(Lv et al., 2015)
Ritonavir	Norvir	1996	HIV infection	~25 nM	−370.98	(Lv et al., 2015)
Indinavir	Crixivan	1996	HIV infection	5.5 nM	−386.65	(Lv et al., 2015)
Nelfinavir	Viracept	1997	HIV infection	30–60 nM	−344.54	(Lv et al., 2015)
Amprenavir	Agenerase	1999	HIV infection	12–80 nM	−359.88	(Lv et al., 2015)
Lopinavir	Lopinavir + ritonavir = kaletra™ [a]	2000	HIV infection	~17 nM	−390.02	(Lv et al., 2015)
Nitazoxanide	Alinia	2002	Giardia lamblia and Ebola virus infection	~ 0.1-3 μM	−246.48	(Jasenosky et al., 2019; Korba et al., 2008; Zhou et al., 2019)
Fosamprenavir	Lexiva Telzir	2003	HIV infection	Prodrug of amprenavir	−331.99	(Lv et al., 2015)
Atazanavir	Reyataz	2003	HIV infection	2.6–5.3 nM	−402.33	(Lv et al., 2015)
Tipranavir	Aptivus	2005	HIV infection	30–70 nM	−415.27	(Lv et al., 2015)
Darunavir	Prezista	2006	HIV infection	1–2 nM	−336.10	(Lv et al., 2015)
Boceprevir	Victrelis	2011	HCV infection	~ 200 nM	−356.67	(Malcolm et al., 2006)
Simeprevir	Olysio	2013	HCV infection	8-28 nM	−383.69	(Izquierdo et al., 2014)
Asunaprevir	Sunvepra (Japan)	2014	HCV infection	1-4 nM	−395.87	(McPhee et al., 2012)

a)Lopinavir + ritonavir = kaletra® with EC_{50} value of 17.1 μM and 8 μM against SARS-CoV and MERS-CoV, respectively (Eynde, 2020).

utilities like the above procedures, potential candidates for treatment of COVID-19 disease are reported. However, future clinical studies in this area would be beneficial to validate these findings.

Disclosure statement

The authors declare no conflict of interest, financial or otherwise.

Authors' contributions

The concept and experimental research plan was designed by Hajiagha Bozorgi A and Mosayebnia M. The valuable collaboration of Prof. Farzad Kobarfard helped us to elaborate on our research ideas. The project administration and data analysis were done by Rezaeianpour R and Hajiagha Bozorgi A. The corresponding author is Dr. Mona Mosayebnia who has written, reviewed and edited this manuscript. All the authors approve the final manuscript for publication.

Funding

This study was funded by Shahid Beheshti University of Medical Sciences (SBMU, 99-24012), Tehran, Iran.

ORCID

Mona Mosayebnia http://orcid.org/0000-0002-6565-2806
Atefeh Hajiagha Bozorgi http://orcid.org/0000-0001-5528-2998
Maliheh Rezaeianpour http://orcid.org/0000-0002-3813-6355
Farzad Kobarfard http://orcid.org/0000-0002-0451-6202

References

Ahmed, S. F., Quadeer, A. A., & McKay, M. R. (2020). Preliminary identification of potential vaccine targets for the COVID-19 Coronavirus (SARS-CoV-2) Based on SARS-CoV Immunological Studies. *Viruses*, *12*(3), 254–268. https://doi.org/10.3390/v12030254

Cao, B., Wang, Y., Wen, D., Liu, W., Wang, J., Fan, G., Ruan, L., Song, B., Cai, Y., Wei, M., Li, X., Xia, J., Chen, N., Xiang, J., Yu, T., Bai, T., Xie, X., Zhang, L., Li, C., … Wang, C. (2020). A Trial of Lopinavir-Ritonavir in Adults Hospitalized with Severe COVID-19. *The New England Journal of Medicine*, *382*(19), 1787–1799. https://doi.org/10.1056/NEJMoa2001282

Carlesso, A., Chintha, C., Gorman, A. M., Samali, A., & Eriksson, L. A. (2019). Merits and pitfalls of conventional and covalent docking in identifying new hydroxyl aryl aldehyde like compounds as human IRE1 inhibitors. *Scientific Reports*, *9*(1), 10. https://doi.org/10.1038/s41598-019-39939-z

Chan, J. F. W., Kok, K. H., Zhu, Z., Chu, H., To, K. K. W., Yuan, S., & Yuen, K. Y. (2020). Genomic characterization of the 2019 novel human-pathogenic coronavirus isolated from a patient with atypical pneumonia after visiting Wuhan. *Emerging Microbes & Infections*, *9*(1), 221–236. https://doi.org/10.1080/22221751.2020.1719902

Chan, J. F. W., To, K. K. W., Tse, H., Jin, D. Y., & Yuen, K. Y. (2013). Interspecies transmission and emergence of novel viruses: Lessons from bats and birds. *Trends in Microbiology*, *21*(10), 544–555. https://doi.org/10.1016/j.tim.2013.05.005

Chandwani, A., & Shuter, J. (2008). Lopinavir/ritonavir in the treatment of HIV-1 infection: A review. *Therapeutics and Clinical Risk Management*, *4*(5), 1023–1033. https://doi.org/10.2147/tcrm.s3285

Chen, N., Zhou, M., Dong, X., Qu, J., Gong, F., Han, Y., Qiu, Y., Wang, J., Liu, Y., Wei, Y., Xia, J., Yu, T., Zhang, X., & Zhang, L. (2020). Epidemiological and clinical characteristics of 99 cases of 2019 novel coronavirus pneumonia in Wuhan, China: A descriptive study. *Lancet*

(London, England), *395*(10223), 507–513. https://doi.org/10.1016/S0140-6736(20)30211-7

Chen, Y., Liu, Q., & Guo, D. (2020). Emerging coronaviruses: Genome structure, replication, and pathogenesis. *Journal of Medical Virology*, *92*(4), 418–423. https://doi.org/10.1002/jmv.25681

Elfiky, A. A. (2020). Anti-HCV, nucleotide inhibitors, repurposing against COVID-19. *Life Sciences*, *248*, 117477–117482. https://doi.org/10.1016/j.lfs.2020.117477

Elfiky, A. A., & Ismail, A. (2019). Molecular dynamics and docking reveal the potency of novel GTP derivatives against RNA dependent RNA polymerase of genotype 4a HCV. *Life Sciences*, *238*, 116958–116990. https://doi.org/10.1016/j.lfs.2019.116958

Enjuanes, L., Almazán, F., Sola, I., & Zuñiga, S. (2006). Biochemical Aspects of Coronavirus Replication and Virus-Host Interaction. *Annual Review of Microbiology*, *60*, 211–230. https://doi.org/10.1146/annurev.micro.60.080805.142157

Eynde, J. J. V. (2020). COVID-19: A brief overview of the discovery clinical trial. *Pharmaceuticals*,13*(4)*, 65–72.

Fauci, A. S., Lane, H. C., & Redfield, R. R. (2020). COVID-19 - Navigating the Uncharted. *The New England Journal of Medicine*, *382*(13), 1268–1269. https://doi.org/10.1056/NEJMe2002387

Furuta, Y., Komeno, T., & Nakamura, T. (2017). Favipiravir (T-705), a broad spectrum inhibitor of viral RNA polymerase. *Proceedings of the Japan Academy. Series B, Physical and Biological Sciences*, *93*(7), 449–463. https://doi.org/10.2183/pjab.93.027

Gao, Y., Yan, L., Huang, Y., Liu, F., Zhao, Y., Cao, L., Wang, T., Sun, Q., Ming, Z., Zhang, L., Ge, J., Zheng, L., Zhang, Y., Wang, H., Zhu, Y., Zhu, C., Hu, T., Hua, T., Zhang, B., … Rao, Z. (2020). Structure of the RNA-dependent RNA polymerase from COVID-19 virus. *Science (New York, N.Y.)*, *368*(6492), 779–782. https://doi.org/10.1126/science.abb7498

Haji Agha Bozorgi, A., & Zarghi, A. (2014). Search for the pharmacophore of histone deacetylase inhibitors using pharmacophore query and docking study. *Iranian Journal of Pharmaceutical Research : IJPR*, *13*(4), 1165–1172.

Han, B., Martin, R., Xu, S., Parvangada, A., Svarovskaia, E. S., Mo, H., & Dvory-Sobol, H. (2019). Sofosbuvir susceptibility of genotype 1 to 6 HCV from DAA-naïve subjects. *Antiviral Research*, *170*, 104574 https://doi.org/10.1016/j.antiviral.2019.104574

Hirashima, S., Suzuki, T., Ishida, T., Noji, S., Yata, S., Ando, I., Komatsu, M., Ikeda, S., & Hashimoto, H. (2006). Benzimidazole derivatives bearing substituted biphenyls as hepatitis C virus NS5B RNA-dependent RNA polymerase inhibitors: Structure-activity relationship studies and identification of a potent and highly selective inhibitor JTK-109. *Journal of Medicinal Chemistry*, *49*(15), 4721–4736. https://doi.org/10.1021/jm060269e

Hoffmann, M., Kleine-Weber, H., Schroeder, S., Krüger, N., Herrler, T., Erichsen, S., Schiergens, T. S., Herrler, G., Wu, N.-H., Nitsche, A., Müller, M. A., Drosten, C., & Pöhlmann, S. (2020). SARS-CoV-2 Cell Entry Depends on ACE2 and TMPRSS2 and Is Blocked by a Clinically Proven Protease Inhibitor. *Cell*, *181*(2), 271–280. https://doi.org/10.1016/j.cell.2020.02.052

Huang, C., Wang, Y., Li, X., Ren, L., Zhao, J., Hu, Y., Zhang, L., Fan, G., Xu, J., Gu, X., Cheng, Z., Yu, T., Xia, J., Wei, Y., Wu, W., Xie, X., Yin, W., Li, H., Liu, M., … Cao, B. (2020). Clinical features of patients infected with 2019 novel coronavirus in Wuhan, China. *Lancet (London, England)*, *395*(10223), 497–506. https://doi.org/10.1016/S0140-6736(20)30183-5

Izquierdo, L., Helle, F., François, C., Castelain, S., Duverlie, G., & Brochot, E. (2014). Simeprevir for the treatment of hepatitis C virus infection. *Pharmacogenomics and Personalized Medicine*, *7*, 241–249. https://doi.org/10.2147/PGPM.S52715

Jasenosky, L. D., Cadena, C., Mire, C. E., Borisevich, V., Haridas, V., Ranjbar, S., Nambu, A., Bavari, S., Soloveva, V., Sadukhan, S., Cassell, G. H., Geisbert, T. W., Hur, S., & Goldfeld, A. E. (2019). The FDA-Approved Oral Drug Nitazoxanide Amplifies Host Antiviral Responses and Inhibits Ebola Virus. *iScience*, *19*, 1279–1290. https://doi.org/10.1016/j.isci.2019.07.003

Jia, H. P., Look, D. C., Shi, L., Hickey, M., Pewe, L., Netland, J., Farzan, M., Wohlford-Lenane, C., Perlman, S., & McCray, P. B. (2005). ACE2 Receptor Expression and Severe Acute Respiratory Syndrome Coronavirus Infection Depend on Differentiation of Human Airway Epithelia. *Journal of Virology*, *79*(23), 14614–14621. https://doi.org/10.1128/JVI.79.23.14614-14621.2005

Jin, Z., Du, X., Xu, Y., Deng, Y., Liu, M., Zhao, Y., Zhang, B., Li, X., Zhang, L., Peng, C., Duan, Y., Yu, J., Wang, L., Yang, K., Liu, F., Jiang, R., Yang, X., You, T., Liu, X., … Yang, H. (2020). Structure of Mpro from SARS-CoV-2 and discovery of its inhibitors. *Nature*, *582*(7811), 289–293. https://doi.org/10.1038/s41586-020-2223-y

Korba, B. E., Elazar, M., Lui, P., Rossignol, J. F., & Glenn, J. S. (2008). Potential for hepatitis C virus resistance to nitazoxanide or tizoxanide. *Antimicrobial Agents and Chemotherapy*, *52*(11), 4069–4071. https://doi.org/10.1128/AAC.00078-08

Li, Q., Guan, X., Wu, P., Wang, X., Zhou, L., Tong, Y., Ren, R., Leung, K. S. M., Lau, E. H. Y., Wong, J. Y., Xing, X., Xiang, N., Wu, Y., Li, C., Chen, Q., Li, D., Liu, T., Zhao, J., Liu, M., … Feng, Z. (2020). Early Transmission Dynamics in Wuhan, China, of Novel Coronavirus-Infected Pneumonia. *The New England Journal of Medicine*, *382*(13), 1199–1207. https://doi.org/10.1056/NEJMoa2001316

Lo, M. K., Jordan, R., Arvey, A., Sudhamsu, J., Shrivastava-Ranjan, P., Hotard, A. L., Flint, M., McMullan, L. K., Siegel, D., Clarke, M. O., Mackman, R. L., Hui, H. C., Perron, M., Ray, A. S., Cihlar, T., Nichol, S. T., & Spiropoulou, C. F. (2017). GS-5734 and its parent nucleoside analog inhibit Filo-, Pneumo-, and Paramyxoviruses. *Scientific Reports*, *7*(1), 1–7. https://doi.org/10.1038/srep43395

Lv, Z., Chu, Y., & Wang, Y. (2015). HIV protease inhibitors: A review of molecular selectivity and toxicity. *HIV/AIDS - Res Palliat Care*, *7*, 95–104.

Macchiagodena, M., Pagliai, M., & Procacci, P. (2020). Inhibition of the main protease 3CL-pro of the coronavirus disease 19 via structure-based ligand design and molecular modeling. *Biomolecules (q-bio.BM)*, 1–28.

Malcolm, B. A., Liu, R., Lahser, F., Agrawal, S., Belanger, B., Butkiewicz, N., Chase, R., Gheyas, F., Hart, A., Hesk, D., Ingravallo, P., Jiang, C., Kong, R., Lu, J., Pichardo, J., Prongay, A., Skelton, A., Tong, X., Venkatraman, S., … Njoroge, F. G. (2006). SCH 503034, a mechanism-based inhibitor of hepatitis C virus NS3 protease, suppresses polyprotein maturation and enhances the antiviral activity of alpha interferon in replicon cells. *Antimicrobial Agents and Chemotherapy*, *50*(3), 1013–1020. https://doi.org/10.1128/AAC.50.3.1013-1020.2006

McMullan, L. K., Flint, M., Chakrabarti, A., Guerrero, L., Lo, M. K., Porter, D., Nichol, S. T., Spiropoulou, C. F., & Albariño, C. (2019). Characterisation of infectious Ebola virus from the ongoing outbreak to guide response activities in the Democratic Republic of the Congo: A phylogenetic and in vitro analysis. *Lancet Infectious Diseases.*, *19*(9), 1023–1032. https://doi.org/10.1016/S1473-3099(19)30291-9

McPhee, F., Sheaffer, A. K., Friborg, J., Hernandez, D., Falk, P., Zhai, G., Levine, S., Chaniewski, S., Yu, F., Barry, D., Chen, C., Lee, M. S., Mosure, K., Sun, L.-Q., Sinz, M., Meanwell, N. A., Colonno, R. J., Knipe, J., & Scola, P. (2012). Preclinical profile and characterization of the hepatitis C virus NS3 protease inhibitor asunaprevir (BMS-650032). *Antimicrobial Agents and Chemotherapy*, *56*(10), 5387–5396. https://doi.org/10.1128/AAC.01186-12

Morse, J. S., Lalonde, T., Xu, S., & Liu, W. R. (2020). Learning from the Past: Possible Urgent Prevention and Treatment Options for Severe Acute Respiratory Infections Caused by 2019-nCoV. *Chembiochem : a European Journal of Chemical Biology*, *21*(5), 730–738. https://doi.org/10.1002/cbic.202000047

Perlman, S., & Netland, J. (2009). Coronaviruses post-SARS: Update on replication and pathogenesis. *Nature Reviews. Microbiology*, *7*(6), 439–450. https://doi.org/10.1038/nrmicro2147

Petrosillo, N., Viceconte, G., Ergonul, O., Ippolito, G., & Petersen, E. (2020). COVID-19, SARS and MERS: Are they closely related? *Clinical Microbiology and Infection*, *26*(6), 729–734. https://doi.org/10.1016/j.cmi.2020.03.026

Pickett, S. D., Mason, J. S., & McLay, L. M. (1996). Diversity profiling and design using 3D pharmacophores: Pharmacophore-derived queries (PDQ). *Journal of Chemical Information and Computer Sciences*, *36*(6), 1214–1223. https://doi.org/10.1021/ci960039g

Pillaiyar, T., Manickam, M., Namasivayam, V., Hayashi, Y., & Jung, S. H. (2016). An overview of severe acute respiratory syndrome-coronavirus

(SARS-CoV) 3CL protease inhibitors: Peptidomimetics and small molecule chemotherapy. *Journal of Medicinal Chemistry*, *59*(14), 6595–6628. https://doi.org/10.1021/acs.jmedchem.5b01461

Sayad, B., Sobhani, M., & Khodarahmi, R. (2020). Sofosbuvir as Repurposed Antiviral Drug Against COVID-19: Why Were We Convinced to Evaluate the Drug in a Registered/Approved Clinical Trial? *Arch Med Res*, *500*, 3–5.

Sheahan, T. P., Sims, A. C., Leist, S. R., Schäfer, A., Won, J., Brown, A. J., Montgomery, S. A., Hogg, A., Babusis, D., Clarke, M. O., Spahn, J. E., Bauer, L., Sellers, S., Porter, D., Feng, J. Y., Cihlar, T., Jordan, R., Denison, M. R., & Baric, R. S. (2020). Comparative therapeutic efficacy of remdesivir and combination lopinavir, ritonavir, and interferon beta against MERS-CoV. *Nature Communications*, *11*(1), 222–235. https://doi.org/10.1038/s41467-019-13940-6

Sidwell, R. W., Bailey, K. W., Wong, M. H., Barnard, D. L., & Smee, D. F. (2005). In vitro and in vivo influenza virus-inhibitory effects of viramidine. *Antiviral Research*, *68*(1), 10–17. https://doi.org/10.1016/j.antiviral.2005.06.003

Sinokrot, H., Smerat, T., Najjar, A., & Karaman, R. (2017). Advanced prodrug strategies in nucleoside and non-nucleoside antiviral agents: A review of the recent five years. Molecules*, 22*, 1736–1754.

Sofia, M. J. (2011). Nucleotide prodrugs for HCV therapy. *Antiviral Chemistry & Chemotherapy*, *22*(1), 23–49. https://doi.org/10.3851/IMP1797

Sofia, M. J., Chang, W., Furman, P. A., Mosley, R. T., & Ross, B. S. (2012). Nucleoside, nucleotide, and non-nucleoside inhibitors of hepatitis C virus NS5B RNA-dependent RNA-polymerase. *Journal of Medicinal Chemistry*, *55*(6), 2481–2531. https://doi.org/10.1021/jm201384j

Tang, B., Bragazzi, N. L., Li, Q., Tang, S., Xiao, Y., & Wu, J. (2020). An updated estimation of the risk of transmission of the novel coronavirus (2019-nCov). *Infectious Disease Modelling*, *5*, 248–255. https://doi.org/10.1016/j.idm.2020.02.001

Wei, C., Mook, R. A., Jr. Robert, A., & Premont, R. T. W. (2018). Niclosamide: Beyond an antihelminthic drug. *Cellular Signalling*, *41*, 89–96. https://doi.org/10.1016/j.cellsig.2017.04.001

Wrapp, D., Wang, N., Corbett, K. S., Goldsmith, J. A., Hsieh, C. L., Abiona, O., Graham, B. S., & McLellan, J. S. (2020). Cryo-EM structure of the 2019-nCoV spike in the prefusion conformation. *Science (New York, N.Y.)*, *367*(6483), 1260–1263. https://doi.org/10.1126/science.abb2507

Wyles, D. L., Rodríguez-Torres, M., Lawitz, E., Shiffman, M. L., Pol, S., Herring, R., Massetto, B., Kanwar, B., Trenkle, J. D., & Pang, P. S. (2014). All-Oral Combination of Ledipasvir. *Vedroprevir, Tegobuvir, and Ribavirin in Treatment- Naive Patients with Genotype 1 HCV Infection David*, *60*, 56–64.

Xu, J., Shi, P.-Y., Li, H., & Zhou, J. (2020). Broad Spectrum Antiviral Agent Niclosamide and Its Therapeutic Potential. *ACS Infectious Diseases*, *6*(5), 909–915. https://doi.org/10.1021/acsinfecdis.0c00052

Yang, P. L., Gao, M., Lin, K., Liu, Q., & Villareal, V. A. (2011). Anti-HCV drugs in the pipeline. *Current Opinion in Virology*, *1*(6), 607–616. https://doi.org/10.1016/j.coviro.2011.10.019

Yao, X., Guo, S., Wu, W., Wang, J., Wu, S., He, S., Wan, Y., Nandakumar, K. S., Chen, X., Sun, N., Zhu, Q., & Liu, S. (2018). Q63, a novel DENV2 RdRp non-nucleoside inhibitor, inhibited DENV2 replication and infection. *Journal of Pharmacological Sciences*, *138*(4), 247–256. https://doi.org/10.1016/j.jphs.2018.06.012

Yin, W., Mao, C., Luan, X., Shen, D.-D., Shen, Q., Su, H., Wang, X., Zhou, F., Zhao, W., Gao, M., Chang, S., Xie, Y.-C., Tian, G., Jiang, H.-W., Tao, S.-C., Shen, J., Jiang, Y., Jiang, H., Xu, Y., … Xu, H. E. (2020). Structural basis for inhibition of the RNA-dependent RNA polymerase from SARS-CoV-2 by remdesivir. *Science (New York, N.Y.)*, *368*(6498), 1499–1504. https://doi.org/10.1126/science.abc1560

Zhou, H., Su, X., Lin, L., Zhang, J., Qi, Q., Guo, F., Xu, F., & Yang, B. (2019). Inhibitory effects of antiviral drug candidates on canine parvovirus in f81 cells. *Viruses*, *11*(8), 742–714. https://doi.org/10.3390/v11080742

Zhu, N., Zhang, D., Wang, W., Li, X., Yang, B., Song, J., Zhao, X., Huang, B., Shi, W., Lu, R., Niu, P., Zhan, F., Ma, X., Wang, D., Xu, W., Wu, G., Gao, G. F., & Tan, W. (2020). A novel coronavirus from patients with pneumonia in China, 2019. *The New England Journal of Medicine*, *382*(8), 727–733. https://doi.org/10.1056/NEJMoa2001017